

Understanding the role of aeolian processes and physical sorting on Martian surface compositions through analysis of spectrally and thermophysically heterogeneous dune fields. Cong Pan and A. Deanne Rogers, Stony Brook University, Department of Geosciences, 255 Earth and Space Science Building, Stony Brook, New York, 11794-2100, Cong.Pan@stonybrook.edu.

Introduction: The composition and particle size distributions within aeolian dunes on Earth are a function of source rock composition(s), comminution during transport and chemical weathering, and aeolian sorting mechanisms [1-2]. The original crystal size and composition of source rock(s) first determine the grain size and composition of sediments derived from those rocks. Preferential comminution and chemical alteration can change the composition of those sediments (as a function of grain size) during transport. Finally, aeolian sorting of particles leads to preferential enrichment of specific materials in certain grain-size fractions (e.g. [3-4]). Grain size, grain shape and density are major factors controlling the aeolian sorting (e.g. [5-6]). Grain sizes are commonly segregated in dunes, with coarse-grained ripple crests and fine-grained troughs. On Earth, three studies of spatial variations of chemical composition within aeolian environments showed that MgO and/or FeO of fine grains are enriched over coarse grains as a result of comminution and sorting [7-9]. On Mars, the “El Dorado” dune field analyzed by the Spirit rover is characterized by olivine-enriched coarse grains and pyroxene-enriched fine grains [10]. Here, we use orbital measurements to examine the compositional and thermophysical heterogeneity within martian dune fields, in an effort to understand whether there are compositional trends with particle size that may place constraints on the source rock compositions, sediment transport history and aeolian sorting.

Data and Methods: We have used Thermal Emission Imaging System (THEMIS) and Compact Reconnaissance Imaging Spectrometer for Mars (CRISM) images to examine composition, THEMIS to derive thermal inertia, and high resolution visible images (CTX, HiRISE) to study dune morphology.

Decorrelation stretch (DCS) images covering sand dunes on the floor of impact craters were first used to locate compositionally heterogeneous dune fields (indicated by color variations within the stretch). Next, these compositional variations of THEMIS daytime images were mapped quantitatively by spectral unit mapping (similar to the methods of [11]) using scene-derived olivine-poor and laboratory olivine emissivity spectra as endmembers. Then, THEMIS and CRISM spectral averages were extracted from compositionally distinct areas within the dune field. THEMIS nighttime thermal inertia images [12] were used to extract thermal

inertia values for compositionally distinct regions within the field. Last, THEMIS daytime (olivine abundance map) and nighttime images were co-registered to perform pixel to pixel analysis between olivine abundance and thermal inertia. Density slicing based on thermal inertia values was used to highlight the spatial variations of thermal and olivine abundance.

Results: Six out of 27 dune fields within impact craters located between 45°N, 42°E to -14.3°N, 60°E were observed to have heterogeneous composition and thermal inertia in this study. TES albedo of these dunes ranges from 0.1 to 0.15 [13] and TES dust cover index range from 0.97 to 0.98 [14], suggesting active removal of dust cover. A sand dune located at 44.26°E, 42.16°N is shown here for example. From CTX imagery (**Figure 1**), we observe larger size and greater areal coverage of ripple and crescents in the northeastern part of the dune (large ripple part), whereas the rest of the dune (small ripple part) is smooth covering smaller size of ripple and crescents, suggesting particle size differences within the dune field. The thermal inertia of the large ripple portion is higher than the small ripple portion, indicating a decrease of effective particle size in small ripple portion (**Figure 2**). Olivine is enriched in large ripple part while poor in the small ripple portion (**Figure 3**). The CRISM mafic parameter browse image also shows stronger olivine index values in the large ripple part (**Figure 4**) and no hydrated minerals were detected. The density slice map (**Figure 5**) confirms the large ripple part has higher thermal inertia than the small ripple part. The positive correlation between thermal inertia and olivine abundance (**Figure 5 and Table 1**) indicates that with the increase of particle size, the olivine abundance increases.

Discussion and Summary: Our results suggest a positive relationship between olivine abundance and particle size within the dune fields studied. The high thermal inertia (larger particle size) portion of the dune exhibits higher olivine abundance and distinct ripple forms, whereas the lower thermal inertia portion of the dune field is relatively olivine poor and morphologically smooth. It is consistent with the observation in “El Dorado” on Mars [10] that olivine was enriched in the coarse grains. However, this trend is opposite of what were observed by [7-9] on Earth.

No hydrated minerals were found within the dune fields, suggesting chemical weathering has limited effect to the trends. One possibility of the variation of

composition may be heterogeneity of sand source that specific grain sizes from different basalt composition were available within the saltation distance of dune. Alternatively, the sediment sources are from a single source that contains large olivine phenocrysts within a finely crystalline matrix.

References: [1]Blatt, H. et al, 1980, New Jersey. [2] Boggs, 1995, New Jersey. [3]Weltje, G.J. and Eynatten H., (2004)*Sedimentary Geology*, 171(1-4), 1-11.[4]Tolosana-delgado, R. and Eynatten, H. , (2009)*Math Geosci*, 41(8), 869-886. [5] Anderson, R.S. and Bunas, K.L. (1993) *Nature*, 365(4480), 740–745. [6]Makse, H.A. (2000) *Eur.Phys.J.E*, 1(2-3), 127–135. [7] Mangold N. et al. (2011)*EPSL*, 310, 233-243. [8] Nesbitt H. W. and Young G.M. (1996) *Sedimentology*, 43(2), 341-358. [9] Xu Z et al. (2011) *J.Geogr.Sci.* 21(6), 1062-1076. [10]Sullivan R. et al. (2008) *JGR*, 113(E6), E06S07. [11] Bandfield, J.L. et al. (2000) *JGR*, 105(E5), 9573–9587. [12] Ferguson, R.L. et al., (2006)*JGR*, 111, E12004. [13] Christensen P.R. et al. (2001)*JGR*, 106(E10), 23823-23871. [14] Ruff, S.W. and Christensen P.R. (2002)*JGR*, 107(E12), 23823-23871

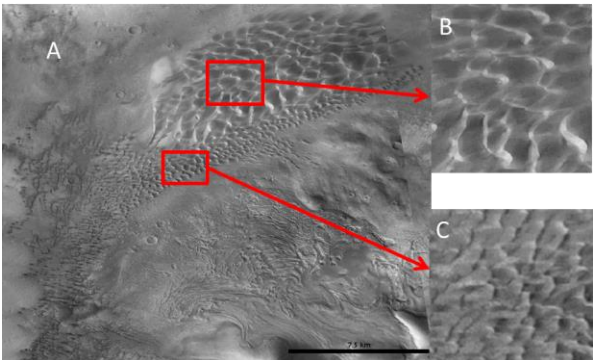


Figure 1. CTX shows geomorphology variation within an intracrater dune field located at 44.26°E, 42.16°N. B and C show the size variations of ripple and crescents.

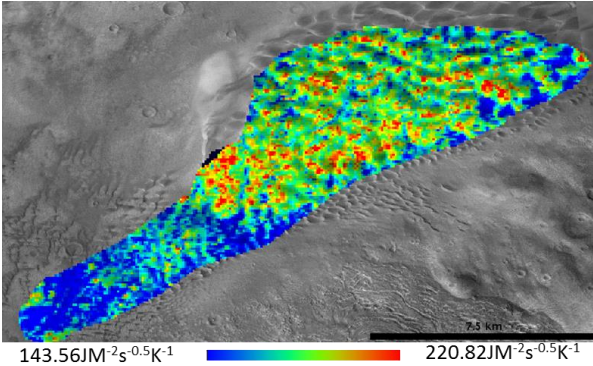


Figure 2. Color stretch map of THEMIS thermal inertia of the dune field. The large ripple part shows

high thermal inertia whereas the small ripple part shows low thermal inertia.

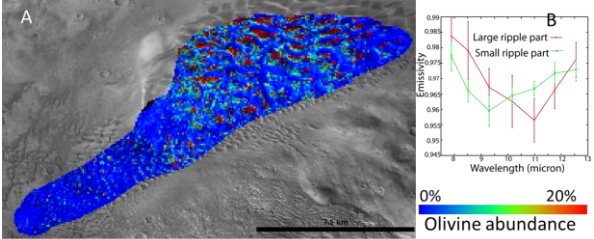


Figure 3. Color stretch map of THEMIS derived olivine abundance (A) and spectra of large ripple and small ripple parts of the dune (B). There is olivine abundance decrease from the large ripple part to the small ripple part.

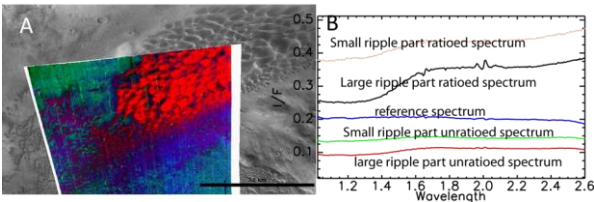


Figure 4. CRISM mafic index map (A) and spectra of large ripple and small ripple parts of the dune (B). The stronger index values and stronger absorption near ~1.2μm of large ripple part refer higher olivine abundance or particle size difference.

Table 1. Average olivine abundance of each thermal inertia range.

Color in Fig. 5	TI range	TI avg	Fo60 abun
	unit: JM-2s-0.5K-1		avg (%)
blue	150-160	155.72	6.48
green	160-170	165.62	7.95
cyan	170-180	175.36	10.42
yellow	180-190	185.27	12.96
purple	190-200	197.12	18.79
red	200-220	208.2	19.69

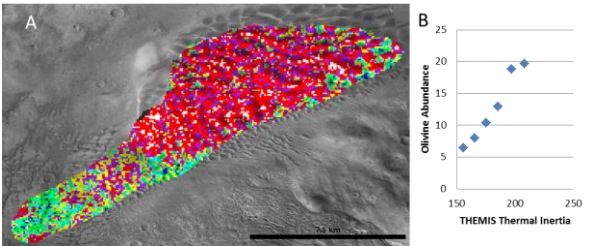


Figure 5. Density sliced THEMIS thermal inertia image (A) and scatter plot of thermal inertia vs. olivine abundance (B). The plot shows that with the increase of thermal inertia (particle size), the olivine abundance increases.